ANL-6406

ANL-6406

Argonne National Laboratory

CALCULATIONS FOR ZPR-VII FLUX-TRAP REACTORS WITH HEAVY WATER-MODERATED CORES

by

E. M. Pennington

ANL-6406
Reactor Technology
(TID-4500, 16th Ed.,
Amended)
AEC Research and
Development Report

ARGONNE NATIONAL LABORATORY
9700 South Cass Avenue
Argonne, Illinois

CALCULATIONS FOR ZPR-VII FLUX-TRAP REACTORS WITH HEAVY WATER-MODERATED CORES

by

E. M. Pennington

Reactor Engineering Division

August 1961

Operated by The University of Chicago
under
Contract W-31-109-eng-38

TABLE OF CONTENTS

FIGURE

LIST OF TABLES

CALCULATIONS FOR ZPR-VII FLUX-TRAP REACTORS WITH HEAVY WATER-MODERATED CORES

by

E. M. Pennington

ABSTRACT

Calculations have been made relating to flux-trap reactors constructed in the ZPR-VII critical assembly having heavy water-moderated cores of THUD or Babcock and Wilcox fuel. The flux-trap regions consisted of heavy water, except for a few light water flux traps with THUD-fueled cores. Various flux ratios and quantities, such as ratios of maximum thermal flux to maximum power density or total core power, are compared for THUD-fueled lattices. In connection with the B-and-W-fueled lattices, which have thin cores with high resonance absorption, a study is made of reactors having cores with $k_\infty < 1$. It is shown that it is possible for a reflected reactor having a core with $k_\infty < 1$ to be critical if $k_\infty/p > 1$, where p is the resonance escape probability, and if the dimensions and material constants involved are of suitable magnitudes.

I. INTRODUCTION

A flux-trap reactor consists of a core having a moderator-filled region at the center (inner reflector) and perhaps also an outer reflector. The thermal flux is highly peaked in the inner reflector, and so it is possible to have higher ratios of maximum thermal flux to maximum power density or total power than is the case for reactors without flux traps. Experimental flux-trap lattices have been constructed in the ZPR-VII critical assembly[1] having heavy water-moderated cores of THUD or Babcock and Wilcox (B and W) fuel.

The THUD fuel consists of pellets of thorium oxide and highly enriched uranium oxide with an atom ratio of thorium to U^{235} of 25:1. The radius of the pellets is 0.2972 cm, and they are clad in thin-walled aluminum tubes, roughly 5 ft long. For the B and W fuel, which also consists of pellets of thorium oxide and enriched uranium oxide, the atom ratio of thorium to U^{235} is 15:1, the radius is 0.3302 cm, and the cladding is also an aluminum tube about 5 ft long. In Reference 2 the properties of both the THUD and B and W fuel pellets and claddings will be described in detail.

Flux-trap reactors containing THUD fuel were constructed with cores having uniform triangular pitches of $2a_0$ or $6a_0$, where a_0 is 0.9525 cm ($\frac{3}{8}$ in.) and is equal to the spacing of the perforations in the grid plates which are used to space the fuel rods. For the $2a_0$ spacing, the cores had various inner radii, outer radii, and heights, as well as an outer reflector consisting mainly of D_2O. The inner reflectors consisted of heavy water or light water with a thin, aluminum cylindrical shell separating H_2O from D_2O in the light water cases. In the case of the $6a_0$ lattices, the cores had various inner radii and heights, but essentially no outer reflector, as the fuel almost reached the wall of the ZPR-VII tank. All $6a_0$ lattices had flux traps consisting of heavy water. Experimental work with the THUD-fueled lattices with heavy water flux traps has been reported briefly in Reference 3. The B-and-W-fueled flux trap reactors had inner and outer reflectors of heavy water, various heights, and cores of $1a_0$ spacing, which were very thin, in some cases being less than 3 cm thick. All lattices had a bottom reflector consisting of an inhomogeneous mixture of D_2O and aluminum structural materials, and no top reflector (except for the forest of fuel rods above the level of the D_2O).

The experimental work on all of the flux-trap lattices will be reported in detail in Reference 4. In the following sections, calculations relating to the lattices with THUD fuel and $2a_0$ spacing, THUD fuel and $6a_0$ spacing, and B and W fuel will be described.

II. CALCULATIONS FOR THUD FUEL WITH $2a_0$ SPACING

A. Heavy Water Flux Traps

Calculations were made for the $2a_0$ lattices with THUD fuel and D_2O flux traps, by means of two-group, one-dimensional diffusion theory with the RE-6 code[5] on UNIVAC. For each set of radial dimensions used, the calculations were repeated with two values of axial buckling corresponding to values of H differing by 15 cm, where H is the critical height. The reactivities were then found from $1 - (1/F)$, where F is given in the output as the number by which k_∞ must be divided to make the reactor critical. Then the calculations were done a third time with axial bucklings interpolated from the first two on the assumption that the reactivity variation with height is proportional to $1/H^3$. In all cases, the third calculation yielded a value of F differing from unity by less than 0.001.

Table I lists the constants which were used in the UNIVAC calculations. The inner reflector was assumed to consist of 98% D_2O and 2% H_2O, whereas the outer reflector was taken to be 97% D_2O, 2% H_2O, and 1% Al to allow roughly for the Al control rod guides. A value of 105 cm was used for the outer radius of the reactor. Note that the two-group age in both reflectors was assumed to be 200 cm^2.[6,7]

Table I

MATERIAL CONSTANTS USED IN THE THUD $2a_0$ CALCULATIONS

	Core	Inner Reflector	Outer Reflector
$\tau(cm^2)$	158.4	200	200
$L^2(cm^2)$	17.688	1856	1445
$D_1(cm)$	1.315	1.251	1.260
$D_2(cm)$	0.8340	0.7774	0.7830
p	0.8577	1	1
k_∞	1.3653	0	0
$B^2(cm^{-2})$	2.0102×10^{-3}		

In Table II are listed the inner core radii R_1, outer core radii R_2, criticality constants F, and heights H for the problems run with UNIVAC. Problem 0 refers to the bare core with dimensions such that the ratio of center flux to total power is maximized. The outer radii of 31.1 and 44.5 cm correspond to values used in the experiments.

Table II

CRITICALITY DATA FOR THUD $2a_0$ CALCULATIONS WITH D_2O FLUX TRAPS

Problem No.	R_1 (cm)	R_2 (cm)	F	H(cm)
0	0	65.69	1	121.4
1	0	31.1	1.000333	128.0
2	4.5	31.1	0.999521	127.7
3	9.0	31.1	0.999637	129.4
4	12.0	31.1	0.999699	132.6
5	15.0	31.1	1.000138	139.0
6	18.0	31.1	0.999958	150.1
7	18.0	44.5	1.000637	104.0
8	24.0	44.5	1.000220	112.5
9	30.0	44.5	0.999035	129.2

Figure 1 is a sketch of the shapes of the fast and thermal fluxes for a typical case. In Table III are given the values of the fluxes, which are denoted by the letters A through H on Figure 1. The fluxes G and H

were taken to be at mesh points rather than where the exact minima and maxima occur. No significance should be attached to the normalization used in Table III.

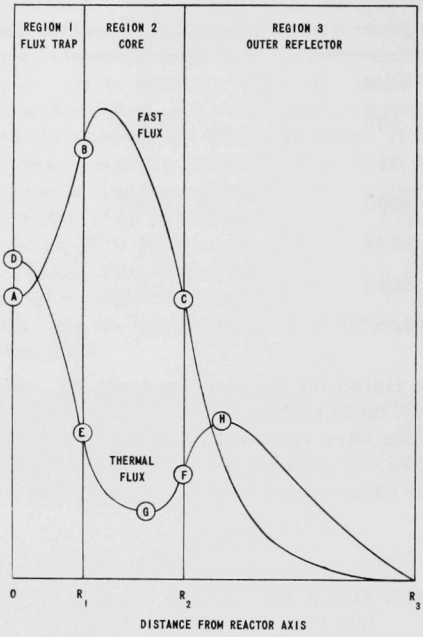

FIG. 1
SKETCH OF THE FLUX SHAPES FOR $2a_0$ LATTICES

Table III

FLUXES FOR THUD $2a_0$ LATTICES WITH D_2O FLUX TRAPS

	Fast Fluxes			Thermal Fluxes				
Problem	A	B	C	D	E	F	G	H
1	137.000		77.259	20.028		31.133	18.571	47.676
2	127.489	131.131	77.615	30.892	25.838	31.362	18.736	47.923
3	111.521	124.500	79.604	49.639	32.000	32.360	19.590	49.435
4	100.049	121.088	82.337	63.699	35.514	32.653	20.894	51.561
5	89.254	119.120	86.423	78.615	39.103	35.944	23.233	55.118
6	78.726	117.408	91.925	93.599	42.899	39.404	27.309	60.341
7	87.960	135.354	86.829	99.958	45.740	33.241	20.964	49.852
8	66.787	135.025	98.008	124.744	50.520	38.309	24.430	58.184
9	52.369	142.022	115.203	152.782	58.026	47.168	32.414	72.295

We turn now to considerations of the magnitudes of the central thermal fluxes when the limitations are maximum power density or total power. Since about 195 Mev of useful energy is produced per fission and one megawatt-sec equals 6.242×10^{18} Mev, the power density is given by

$$\frac{195\Sigma_f \Phi}{6.242 \times 10^{18}} \frac{\text{Mw}}{\text{cm}^3} = \frac{\Sigma_f \Phi}{3.2 \times 10^{16}} \frac{\text{Mw}}{\text{cm}^3} ,$$

where Σ_f is the macroscopic fission cross section and Φ is the thermal flux. Thus for a bare reactor, the ratio of the central flux to maximum power density is given by $(3.2 \times 10^{16})/\Sigma_f$, whereas for a flux-trap reactor this ratio is $\left(\frac{3.2 \times 10^{16}}{\Sigma_f}\right)\left(\frac{\Phi_2(0)}{\bar{\Phi}_{2CM}}\right)$, where $\Phi_2(0)$ is the thermal flux at the center of the reactor and Φ_{2CM} is the maximum thermal flux in the core. The ratio of central flux to total power for a bare cylindrical reactor is given by $\left(\frac{3.2 \times 10^{16}}{\Sigma_f}\right)\left(\frac{\pi j_{01}}{4J_1(j_{01})}\right)\left(\frac{1}{\pi R^2 H}\right)$, where R is the radius of the reactor and H its height. For a flux-trap reactor the corresponding ratio is $\left(\frac{3.2 \times 10^{16}}{\Sigma_f}\right)\left(\frac{\Phi_2(0)}{\bar{\Phi}_{2C}}\right)\left(\frac{1}{\pi(R_2^2 - R_1^2)H}\right)$, where $\bar{\Phi}_{2C}$ is the average thermal flux in the core. Note that for a bare reactor the ratio of central flux to total power is proportional to $1/(R^2H)$. Thus R and H can be chosen to maximize this ratio under the restriction that

$$B^2 = \frac{\pi^2}{H^2} + \frac{j_{01}^2}{R^2} .$$

This gives

$$H = \sqrt{2}\, \pi R / j_{01}$$

and

$$\left(\frac{3.2 \times 10^{16}}{\Sigma_f}\right)\left(\frac{B^3}{6\sqrt{3}\, \pi j_{01} J_1(j_{01})}\right) = \left(\frac{3.2 \times 10^{16}}{\Sigma_f}\right)(0.024533B^3)$$

as the maximum value of the ratio of central flux to total power.

In Table IV are given flux ratios and power-limited fluxes for the $2a_0$ lattices. In this table, I_{2C} is the integral of the thermal flux over the core volume, R is the value of $\Phi_2(0)/I_{2C}$ divided by the corresponding value for a bare reactor of optimum dimensions, and other symbols have been defined previously. The central flux is given for a maximum power density

of 100 watts and for a total power of 100 Mw. These values have no great significance and are merely used to yield definite numbers for the central fluxes rather than numbers involving power as a factor. They were also used by Ergen[8] in his study of spherical flux-trap reactors with very thin cores.

Table IV shows that the flux-trap reactors with small flux-trap radius have a smaller central flux than a bare reactor if maximum power density is the limitation considered. This is due to the fact that little peaking takes place in a flux trap of small radius. For this reason the peaking in the core near the boundary between the core and the outer reflector becomes more significant. However, the ratio $\Phi_2(0)/\Phi_{2CM}$ increased steadily with flux-trap radius over the range of radii considered and reached a value of 2.633 for an internal radius of 30 cm.

Table IV

FLUX RATIOS AND POWER-LIMITED FLUXES FOR $2a_0$ LATTICES WITH D_2O FLUX TRAPS

Problem	$\frac{\Phi_2(0)}{\Phi_{2CM}}$	$\frac{\Phi_2(0)}{\bar{\Phi}_{2C}}$	$\frac{\Phi_2(0)}{I_{2C}}$ ($cm^{-3} \times 10^{-6}$)	R	$\Phi_2(0)$* [$n/(cm^2)(sec) \times 10^{14}$]	$\Phi_2(0)$** [$n/(cm^2)(sec) \times 10^{14}$]
0	1	3.6381	2.2111	1	1.053	2.328
1	0.6433	1.503	3.864	1.748	0.6774	4.069
2	0.9850	2.271	5.979	2.704	1.037	6.296
3	1.534	3.415	9.479	4.287	1.615	9.981
4	1.794	4.070	11.87	5.368	1.889	12.50
5	2.010	4.527	13.97	6.318	2.117	14.71
6	2.182	4.672	15.40	6.965	2.298	16.22
7	2.185	6.271	11.59	5.242	2.301	12.20
8	2.469	6.638	13.37	6.047	2.600	14.08
9	2.633	6.262	14.28	6.458	2.773	15.04

*maximum power density = 100 watts/cm^3

**total power = 100 Mw

The ratio of the central flux for the flux-trap reactor to the central flux for a bare reactor of optimum dimensions in the total power-limited case is 1.748 for the reactor with external reflector only and core radius 31.1 cm, and increases rapidly as the flux-trap radius is increased. Of course, both inner and outer reflectors contribute to this increase, whereas the outer reflector can be a hindrance in the power-density-limited case.

Table V gives the neutron inventory for a typical $2a_0$ lattice, namely, that of Problem 7.

Table V

NEUTRON INVENTORY FOR A TYPICAL $2a_0$ LATTICE WITH D_2O FLUX TRAP

Fast Neutrons

Region	Source	Total Removals	Total Leakage	Axial Leakage	Radial Leakage	
					Inner Radius	Outer Radius
1	0	0.07222	-0.07222	0.01318	0	-0.08540
2	1	0.55901	0.44099	0.08080	0.08540	0.27479
3	0	0.22615	-0.22615	0.04127	-0.27479	0.00737
Total	1	0.85738	0.14262	0.13525	0.00737	

Thermal Neutrons

Region	Source	Absorptions	Total Leakage	Axial Leakage	Radial Leakage	
					Inner Radius	Outer Radius
1	0.07222	0.00324	0.06898	0.00549	0	0.06349
2	0.47946	0.62862	-0.14916	0.01015	-0.06349	-0.09582
3	0.22615	0.03857	0.18758	0.05086	0.09582	0.04090
Total	0.77783	0.67043	0.10740	0.06650	0.04090	

The critical dimensions calculated for the $2a_0$ lattices are in reasonable agreement with the experimental ones which will be reported in Reference 4. Of course, the value of H in the UNIVAC problems is to be compared with the experimental core height plus the axial reflector savings. The calculated thermal fluxes differ somewhat from the ones obtained by foil activation in that there is a tendency for the theoretical thermal fluxes to be higher than the experimental in the outer reflector and lower than the experimental at the flux-trap center. It is possible that the use of different reflector constants could improve this situation. Perhaps the value of 200 cm^2 used for the age in both reflectors is too high, and also the values used for L^2 in the reflectors may not be very accurate. The values of L^2 depend strongly on light water impurity and, in the case of the outer reflector, on the inhomogeneity due to the presence of Al control rod guides. However, because of limitations on machine time, no calculations were done with different reflector parameters.

B. Light Water Flux Traps

For the $2a_0$ lattices with H_2O flux trap, calculations were performed using the RE-122 code on the IBM-704 computer. This code is essentially the RE-6 UNIVAC code rewritten for the 704. In rewriting the code, provision was made for iteration on axial buckling to make the reactor critical.

Thus it was necessary to do only one problem for a given set of radial dimensions. The convergence criterion used was such that F should differ from unity by less than 0.0005.

The core and outer reflector constants used in the RE-122 problems were those given in Table I. For the inner H_2O reflector the values τ = 33 cm^2, L^2 = 8.025 cm^2, D_1 = 1.19 cm, and D_2 = 0.1581 cm were used. Experimental inner core radii calculated by assigning the area of a unit cell to each fuel rod are a little larger than the inner radius of the Al thimble. In general, the core was considered to extend right up to the inner Al thimble radius in the RE-122 calculations, although in problem 6 below, a thin D_2O region having the constants of the inner reflector in Table I was inserted between the flux trap and core. Otherwise problem 6 is the same as problem 5. Table VI lists the inner and outer flux trap radii R_1 and R_2 of the RE-122 problems along with the converged values of F and corresponding heights H. The two values of R_1 in problem 6 refer to the inner and outer radii of the above-mentioned thin D_2O region.

Table VI

CRITICALITY DATA FOR THUD $2a_0$ CALCULATIONS WITH H_2O FLUX TRAPS

Problem No.	R_1 (cm)	R_2 (cm)	F	H (cm)
1	0	27.61	1.000457	148.2
2	2.54	27.61	0.999979	145.5
3	5.08	30.50	1.000432	140.1
4	5.08	29.04	1.000061	149.8
5	3.175	27.61	1.000217	147.0
6	3.175, 4.36	27.61	1.000132	148.6

Table VII for the H_2O flux traps is analogous to Table III for the D_2O flux traps, and also the notation of Figure 1 is used in specifying the fluxes. The two values of B and E for problem 6 correspond to the inner and outer radii of the thin D_2O region.

Table VIII gives the same quantities for H_2O flux traps as are given in Table IV for D_2O flux traps. The notation in the two tables is identical.

The maximum value of $\Phi_2(0)/\Phi_{2CM}$ in Table VIII is 2.753 for problem 3, which is a little higher than the highest value, 2.633, for the D_2O flux traps of Table IV. Also, the ratio of central flux for the flux-trap reactor to central flux for a bare reactor of optimum dimensions in the total power limited case attains a value of 8.371 in problem 4, which is higher than the highest value obtained for the D_2O flux traps studied, namely, 6.965.

Table VII

FLUXES FOR THUD $2a_0$ LATTICES WITH H_2O FLUX TRAPS

Problem	Fast Fluxes			Thermal Fluxes				
	A	B	C	D	E	F	G	H
1	128.95		75.875	18.923		31.683	18.212	48.794
2	1613.5	1694.5	1077.5	883.16	440.59	449.00	262.25	689.66
3	1030.5	1245.6	897.39	1190.7	432.54	370.00	216.59	570.80
4	1107.1	1337.7	980.24	1279.7	465.30	409.42	238.07	634.02
5	1512.3	1631.8	1072.9	1062.8	470.04	447.78	261.89	688.63
6	1449.2	1563.6	1080.6	1081.6	535.03	451.83	264.59	695.63
		1639.8			448.26			

Table VIII

FLUX RATIOS AND POWER-LIMITED FLUXES FOR $2a_0$ LATTICES WITH H_2O FLUX TRAPS

Problem	$\frac{\Phi_2(0)}{\Phi_{2CM}}$	$\frac{\Phi_2(0)}{\bar{\Phi}_{2C}}$	$\frac{\Phi_2(0)}{I_{2C}}$ $(cm^{-3} \times 10^{-6})$	R	$\Phi_2(0)$* $[n/(cm^2)(sec) \times 10^{14}]$	$\Phi_2(0)$** $[n/(cm^2)(sec) \times 10^{14}]$
1	0.5973	1.420	4.000	1.809	0.6290	4.212
2	1.967	4.545	13.15	5.948	2.071	13.85
3	2.753	7.328	18.42	8.328	2.899	19.39
4	2.750	7.121	18.51	8.371	2.896	19.49
5	2.261	5.441	15.66	7.083	2.381	16.49
6	2.394	5.472	15.78	7.135	2.521	16.61

*Maximum power density = 100 watts/cm^3

**Total power = 100 Mw

The neutron inventory for problem 3 is given in Table IX.

Critical heights calculated for the $2a_0$ lattices with light water flux traps are not in very good agreement with the experimental values.[9,4] The calculations predict much lower critical heights relative to the reactor with no flux trap (problem 1) than are found experimentally. Perhaps some of the difficulty is due to the use of diffusion theory, which might be expected to be poor near the interface between core and flux trap, at which the reactor composition changes so drastically, as does the slope of the thermal flux.

Table IX

NEUTRON INVENTORY FOR A TYPICAL $2a_0$ LATTICE WITH H_2O FLUX TRAP

Fast Neutrons

Region	Source	Total Removals	Total Leakage	Axial Leakage	Radial Leakage	
					Inner Radius	Outer Radius
1	0	0.06112	-0.06112	0.00101	0	-0.06213
2	1	0.53843	0.46157	0.04292	0.06213	0.35652
3	0	0.31968	-0.31968	0.03217	-0.35652	0.00467
Total	1	0.91923	0.08077	0.07610	0.00467	

Thermal Neutrons

Region	Source	Absorp-tions	Total Leakage	Axial Leakage	Radial Leakage	
					Inner Radius	Outer Radius
1	0.06112	0.02475	0.03637	0.00010	0	0.03627
2	0.46181	0.62849	-0.16668	0.00559	-0.03627	-0.13600
3	0.31968	0.07576	0.24392	0.05509	0.13600	0.05283
Total	0.84261	0.72900	0.11361	0.06078	0.05283	

III. CALCULATIONS FOR THUD FUEL WITH $6a_0$ SPACING

For the $6a_0$ lattices, calculations were done analytically using a Fortran program, RE 240,* for the IBM-704. This program uses two-group diffusion theory for an annular core with an inner reflector but no outer reflector. The equations which were used in writing the program along with a description of the input and output are given in the Appendix.

Material constants used in the RE-240 calculations are listed in Table X. Note that the calculations were done for an inner reflector with either 2% H_2O impurity or pure D_2O, and also with a reflector age of 200 cm^2 or a calculated value.

Table X

MATERIAL CONSTANTS USED IN THE THUD $6a_0$ CALCULATIONS

		Inner Reflector			
		2% H_2O		Pure D_2O	
	Core	Case I	Case II	Case III	Case IV
$\tau(cm^2)$	150.7	200	122	200	127
L^2 (cm^2)	173.1	1856	1856	3×10^4	3×10^4
D_1 (cm)	1.266	1.251	1.251	1.251	1.251
D_2 (cm)	0.794	0.7774	0.7774	0.8418	0.8418
p	0.9852	1	1	1	1
k_∞	1.4130	0	0	0	0
B^2 (cm^{-2})	1.1660×10^{-3}				

Table XI contains the critical dimensions for the problems run for all four cases of inner reflector constants given in Table X. In Table XI, R_1 and R_2 are the inner and outer core radii, respectively, and H is the height. Problem 00 refers to the bare reactor with critical dimensions which yields the maximum ratio of central flux to total power.

Table XI

CRITICAL DIMENSIONS FOR THUD $6a_0$ CALCULATIONS

			R_1 (cm)			
Problem	R_2 (cm)	H (cm)	Case I	Case II	Case III	Case IV
00	86.25	159.36	0	0	0	0
0	105	124.04	0	0	0	0
1	105	126.89	9.15	9.82	10.41	11.33
2	105	132.25	15.21	15.81	17.27	18.15
3	105	141.42	21.45	21.93	24.32	25.11
4	105	160.11	28.94	29.31	32.80	33.50
5	105	196.73	36.30	36.59	41.17	41.81

*Written by J. Rathbun, student aide in Reactor Engineering Division during summer of 1960.

In Table XII the values of fluxes from the RE-240 output for all four sets of reflector constants are given. The notation A, B, D, E for the fluxes is the same as used in Figure I and Table III. For Problem 00 and 0, A = B = 368.37 and D = E = 553.03.

Table XII

FLUXES FOR THUD $6a_0$ LATTICES

	Case I				Case II			
Problem	A	B	D	E	A	B	D	E
1	271.00	303.79	598.70	565.94	228.82	280.09	656.37	597.45
2	195.41	263.55	612.39	552.06	146.49	238.35	678.26	585.29
3	134.85	234.51	606.88	531.12	89.640	210.85	665.46	561.68
4	85.257	212.16	587.42	509.01	48.980	190.48	630.53	535.88
5	54.599	198.74	569.06	495.33	27.084	178.24	597.02	519.33
	Case III				Case IV			
Problem	A	B	D	E	A	B	D	E
1	256.85	297.42	621.10	578.09	211.39	273.04	681.58	610.37
2	176.30	257.40	650.05	569.90	127.73	233.13	714.31	602.09
3	115.39	230.02	659.65	554.30	73.660	207.97	713.86	583.26
4	68.362	209.52	661.56	538.76	37.463	189.53	699.75	564.11
5	40.829	196.82	672.61	531.67	19.182	177.87	696.67	554.15

Table XIII gives the same quantities relating to power considerations for the $6a_0$ lattices as were given in Table IV for the $2a_0$ lattices.

Table XIII

FLUX RATIOS AND POWER-LIMITED FLUXES FOR $6a_0$ LATTICES

Problem	$\frac{\Phi_2(0)}{\Phi_{2CM}}$	$\frac{\Phi_2(0)}{\Phi_{2C}}$	$\frac{\Phi_2(0)}{I_{2C}}$ $(cm^{-3} \times 10^{-6})$	R	$\Phi_2(0)^*$ $[n/(cm^2)(sec) \times 10^{14}]$	$\Phi_2(0)^{**}$ $[n/(cm^2)(sec) \times 10^{14}]$
00	1	3.638	0.9768	1	12.02	11.74
0	1	3.638	0.8468	0.8669	12.02	10.17
			Case I			
1	1.058	3.939	0.9031	0.9245	12.71	10.85
2	1.109	4.029	0.8984	0.9197	13.32	10.79
3	1.143	3.992	0.8505	0.8707	13.73	10.22
4	1.154	3.864	0.7541	0.7720	13.87	9.061
5	1.149	3.774	0.6240	0.6388	13.81	7.497
			Case II			
1	1.099	4.318	0.9911	1.015	13.20	11.91
2	1.159	4.462	0.9967	1.020	13.93	11.98
3	1.185	4.378	0.9346	0.9568	14.24	11.23
4	1.177	4.148	0.8112	0.8305	14.14	9.747
5	1.150	3.928	0.6561	0.6717	13.82	7.883
			Case III			
1	1.074	4.086	0.9389	0.9612	12.90	11.28
2	1.141	4.276	0.9594	0.9822	13.71	11.53
3	1.190	4.340	0.9362	0.9584	14.30	11.25
4	1.228	4.352	0.8696	0.8903	14.75	10.45
5	1.265	4.425	0.7674	0.7856	15.20	9.220
			Case IV			
1	1.117	4.484	1.032	1.057	13.42	12.40
2	1.186	4.699	1.057	1.082	14.25	12.70
3	1.224	4.696	1.017	1.041	14.71	12.22
4	1.240	4.603	0.9241	0.9460	14.90	11.10
5	1.257	4.583	0.7993	0.8183	15.10	9.604

* Maximum power density = 100 watts/cm^3

** Total power = 100 Mw.

For the $6a_0$ flux-trap reactors, the peaking in the flux trap was not very great, and the largest value of $\Phi_2(0)/\Phi_{2CM}$ for any of the cases studied was 1.265. However, for the power-density-limited case, larger values of central flux are possible than for the $2a_0$ lattices. This is because the maximum flux is inversely proportional to the macroscopic fission cross section, which is over ten times as large for the $2a_0$ core as for the $6a_0$ core. Thus the much better peaking in the $2a_0$ case does not cancel the effect of the smaller fission cross section of the $6a_0$ core when power density is the limiting consideration.

For the total-power-limited case, the central flux was less than that for the bare reactor of optimum dimensions in most of the $6a_0$ problems studied. In the case of the $2a_0$ lattices, the improvement over the optimum bare lattice was almost by a factor of seven in one problem. However, this comparison is not entirely fair to the $6a_0$ lattices. The lattices studied in the $6a_0$ case had cores which were somewhat "shorter and fatter" than the optimum dimensions, as can be seen by comparing values of R_2 and H for problems 00 and 0 in Table XI. Also, the $2a_0$ lattices had outer reflectors, which help to increase the central flux in the total-power-limited case, whereas the $6a_0$ lattices were externally bare. Nevertheless, the much more highly absorbing $2a_0$ core produces much larger flux gradients at the core boundaries than the $6a_0$ core. The best $2a_0$ lattices studied here have a higher central flux in the total-power-limited case than the best $6a_0$ lattices in spite of the fact that the $6a_0$ lattices are favored by a factor larger than ten in the fission cross sections.

The neutron inventory for Problem 3 of the $6a_0$ lattices is given in Table XIV.

Table XIV

NEUTRON INVENTORY FOR A TYPICAL $6a_0$ LATTICE

Case I

Fast Neutrons

Region	Source	Total Removals	Total Leakage	Axial Leakage	Radial Leakage	
					Inner Radius	Outer Radius
1	0	0.03159	-0.03159	0.00312	0	-0.03471
2	1	0.82475	0.17525	0.06134	0.03471	0.07920
Total	1	0.85634	0.14366	0.06446	0.07920	

Thermal Neutrons

Region	Source	Absorptions	Total Leakage	Axial Leakage	Radial Leakage	
					Inner Radius	Outer Radius
1	0.03159	0.00665	0.02494	0.00610	0	0.01884
2	0.81254	0.69726	0.11528	0.05956	-0.01884	0.07456
Total	0.84413	0.70391	0.14022	0.06566	0.07456	

Table XIV (Cont'd.)

Case II

Fast Neutrons

Region	Source	Total Removals	Total Leakage	Axial Leakage	Radial Leakage	
					Inner Radius	Outer Radius
1	0	0.04329	-0.04329	0.00261	0	-0.04590
2	1	0.81447	0.18553	0.06057	0.04590	0.07906
Total	1	0.85776	0.14224	0.06318	0.07906	

Thermal Neutrons

Region	Source	Absorptions	Total Leakage	Axial Leakage	Radial Leakage	
					Inner Radius	Outer Radius
1	0.04329	0.00756	0.03573	0.00692	0	0.02881
2	0.80242	0.69726	0.10516	0.05956	-0.02881	0.07441
Total	0.84571	0.70482	0.14089	0.06648	0.07441	

Case III

Fast Neutrons

Region	Source	Total Removals	Total Leakage	Axial Leakage	Radial Leakage	
					Inner Radius	Outer Radius
1	0	0.03816	-0.03816	0.00377	0	-0.04193
2	1	0.81657	0.18343	0.06073	0.04193	0.08077
Total	1	0.85473	0.14527	0.06450	0.08077	

Thermal Neutrons

Region	Source	Absorptions	Total Leakage	Axial Leakage	Radial Leakage	
					Inner Radius	Outer Radius
1	0.03816	0.00062	0.03754	0.00918	0	0.02836
2	0.80448	0.69726	0.10722	0.05956	-0.02836	0.07602
Total	0.84264	0.69788	0.14476	0.06874	0.07602	

Case IV

Fast Neutrons

Region	Source	Total Removals	Total Leakage	Axial Leakage	Radial Leakage	
					Inner Radius	Outer Radius
1	0	0.05104	-0.05104	0.00320	0	-0.05424
2	1	0.80507	0.19493	0.05987	0.05424	0.08082
Total	1	0.85611	0.14389	0.06307	0.08082	

Thermal Neutrons

Region	Source	Absorptions	Total Leakage	Axial Leakage	Radial Leakage	
					Inner Radius	Outer Radius
1	0.05104	0.00071	0.05033	0.01056	0	0.03977
2	0.79315	0.69726	0.09589	0.05956	-0.03977	0.07610
Total	0.84419	0.69797	0.14622	0.07012	0.07610	

Critical dimensions calculated for the $6a_0$ lattices with $L^2 = 1856\ cm^2$ in the reflector are in fair agreement with experimental values, although the maximum flux-trap radius studied experimentally was less than the radii of Problems 4 and 5. Since the thermal flux in the flux trap is peaked only a little over the J_0 shape of a bare reactor, the flux shapes do not provide much opportunity to compare theory and experiment.

IV. TWO-GROUP TREATMENT OF A CRITICAL SLAB REACTOR STRESSING THE CASE FOR WHICH $k_\infty < 1$

An interesting feature of the la_0 lattices with B and W fuel is the fact that, because of very high resonance absorption, the value of k_∞ is less than unity. It is commonly believed that it is not possible to build a critical reactor having a core with $k_\infty < 1$. However, this statement is true only for a bare reactor. If a reflected reactor has a core with $k_\infty < 1$, but $k_\infty/p > 1$, it may be possible for it to be critical. Using two-group theory for a slab reactor with an infinitely thick reflector on both sides of the core, a study has been made of the variation of the resonance escape probability p with core half-thickness H necessary to make the reactor critical. Illustrative numerical calculations have been performed for the case in which the perpendicular buckling is zero. For the case in which $k_\infty < 1$, the value of p increases rapidly from zero as H increases, reaches a maximum, and slowly decreases to an asymptotic value as $H \to \infty$. Thus for a certain range of p values, there are two critical values of H. This behavior can be explained physically as follows. For very thin cores, p is small and k_∞/p is large, since a large percentage of neutrons produced are absorbed in the reflector. As the core becomes thicker, this effect becomes less important and so p increases. Of the neutrons thermalized in the core, only $k_\infty (< 1)$ are thermalized for each thermal neutron absorbed in the core. Thus a considerable fraction of the fast neutrons produced in the core must be thermalized in the reflector and leak back to the core to maintain criticality. As the core gets thicker, a smaller fraction of neutrons are thermalized in the reflector, and so p decreases and k_∞/p increases to sustain criticality. At first it might be thought that p would decrease to zero again for very large H, since only a small part of the core is near the reflector. However, the thermal flux increases exponentially from the center of the core, and so a reasonable number of neutrons are produced near enough to the core boundary to slow down in the reflector even for very large H. Thus, if H is large, p approaches a finite asymptotic value rather than zero. The theory used for these considerations is given in the following paragraphs.

We start with the usual two-group diffusion equation for core and reflector, namely,

$$D_{1c} \frac{d^2\phi_{1c}}{dx^2} - \frac{D_{1c}}{\tau_c}(1 + \tau_c B_1^2)\phi_{1c} + \frac{k_\infty}{p}\frac{D_{2c}}{L_c^2}\phi_{2c} = 0 \qquad (1)$$

$$D_{2c} \frac{d^2\phi_{2c}}{dx^2} - \frac{D_{2c}}{L_c^2}(1 + L_c^2 B_1^2)\phi_{2c} + \frac{pD_{1c}}{\tau_c}\phi_{1c} = 0 \qquad (2)$$

$$D_{1r} \frac{d^2\phi_{1r}}{dx^2} - \frac{D_{1r}}{\tau_r}(1 + \tau_r B_\perp^2)\phi_{1r} = 0 \qquad (3)$$

$$D_{2r} \frac{d^2\phi_{2r}}{dx^2} - \frac{D_{2r}}{L_r^2}(1 + L_r^2 B_\perp^2)\phi_{2r} + \frac{D_{1r}}{\tau_r}\phi_{1r} = 0 \qquad (4)$$

where the notation is standard. The solutions of these equations, which have zero slope at the middle of the core ($x = 0$) and vanish for $x \to \infty$, are:

$$\phi_{1c} = AX + CY$$

$$\phi_{2c} = S_1 AX + S_2 CY$$

$$\phi_{1r} = FZ_1$$

$$\phi_{2r} = S_3 FZ_1 + GZ_2$$

where

$$X = \cos lx \quad ,$$

$$Y = \cosh mx \quad ,$$

$$Z_1 = e^{-p_1 x} \quad ,$$

$$Z_2 = e^{-p_2 x} \quad ,$$

$$l^2 = \mu^2 - B_\perp^2 \quad ,$$

$$m^2 = \nu^2 + B_\perp^2 \quad ,$$

$$p_1^2 = 1/\tau_r + B_\perp^2 \quad ,$$

$$p_2^2 = 1/L_r^2 + B_\perp^2 \quad ,$$

$$S_1 = \frac{pD_{1c}}{\tau_c D_{2c}\left(\frac{1}{L_c^2} + \mu^2\right)} \; ;$$

$$S_2 = \frac{pD_{1c}}{\tau_c D_{2c}\left(\frac{1}{L_c^2} - \nu^2\right)} \; ;$$

$$S_3 = \frac{D_{1r}}{\tau_r D_{2r}\left(\frac{1}{L_r^2} - \frac{1}{\tau_r}\right)} \; ,$$

and μ^2 and ν^2 are defined in the appendix.

The critical determinant is found from the usual conditions that

$$\phi_{1c} = \phi_{1r}$$

$$\phi_{2c} = \phi_{2r}$$

$$D_{1c} \frac{d\phi_{1c}}{dx} = D_{1r} \frac{d\phi_{1r}}{dx}$$

and

$$D_{2c} \frac{d\phi_{2c}}{dx} = D_{2r} \frac{d\phi_{2r}}{dx}$$

with all functions being evaluated at x = H. In order to simplify the formulae, we take

$$D_{1c} = D_{1r}$$

$$D_{2c} = D_{2r}$$

and

$$\tau_r = \tau_c = \tau \quad .$$

Then the critical determinant may be evaluated and written as follows:

$$p = \frac{(m \tanh mH + \ell \tan \ell H)\frac{1}{\tau p_1 (p_1 + p_2)}}{\left[m \tanh mH\left(\frac{1}{1+\tau\mu^2} + \frac{L_c^2}{\tau(1+L_c^2\mu^2)}\frac{p_2}{p_1}\right) - \ell \tan \ell H\left(\frac{L_c^2}{\tau(1+L_c^2\mu^2)} + \frac{1}{1+\tau\mu^2}\frac{p_2}{p_1}\right) - (m \tanh mH)(\ell \tan \ell H)\frac{(L_c^2+\tau+2L_c^2\tau\mu^2)}{k_\infty \tau p_1} + \frac{L_c^2+\tau+2L_c^2\tau\mu^2}{k_\infty \tau} p_2\right]} \quad (5)$$

The above equation was used in numerical calculations for $B_\perp^2 = 0$. For $B_\perp^2 = 0$ and $k_\infty < 1$, $\ell \tan \ell H$ becomes $-\alpha \tanh \alpha H$ with $\ell^2 = \mu^2 = -\alpha^2$, where α^2 is positive. Also, X becomes $\cosh \alpha x$. The behavior of p as a function of H for $k_\infty < 1$ has been described above. For $B_\perp^2 = 0$ and $k_\infty = 1$, $\mu = 0$ and p is given by

$$p(B_\perp^2 = 0, k_\infty = 1) = \frac{(\nu \tanh \nu H)\left(\frac{L_r}{L_r + \sqrt{\tau}}\right)}{(\nu \tanh \nu H)\left(1 + \frac{L_c^2}{L_r\sqrt{\tau}}\right) + \left(\frac{L_c^2 + \tau}{\tau L_r}\right)} \quad .$$

Thus, for $k_\infty = 1$, p increases from zero with increasing H and soon attains an asymptotic value. This is not surprising since an average of one thermal neutron is thermalized for each thermal neutron absorbed in the core whether the thermalization takes place in the core or in the

reflector. For $k_\infty > 1$, which is the case usually considered, $\mu > 0$ and p increases from zero with increasing H and attains a value of unity for a value of H less than $(\pi/2\mu)$. In this case, there are other intervals of H where $H > (\pi/2\mu)$ which yield a value of p between 0 and 1, but these values do not have physical significance because they yield fluxes which are not always positive. For the case $k_\infty < 1$, a sufficient condition for the fluxes to be positive is $S_1 > 0$ and $S_2 < 0$, which is true for most sets of reasonable values of the constants involved.

The following sets of constants were used to calculate p as a function of H: $B_1^2 = 0$, $L_r^2 = 1000\ cm^2$, $\tau = 125\ cm^2$, $L_c^2 = 4\ cm^2$, $k_\infty = 0.95$, 1, and 1.10. Table XV gives the results.

Table XV

p AS A FUNCTION OF H FOR THREE VALUES OF k_∞

H	$k_\infty = 0.95$		$k_\infty = 1$		$k_\infty = 1.1$	
(cm)	p	k_∞/p	p	k_∞/p	p	k_∞/p
0	0	∞	0	∞	0	∞
0.1	0.30813	3.0831	0.32445	3.0821	0.35701	3.0811
0.2	0.42617	2.2292	0.44889	2.2277	0.49431	2.2253
0.5	0.55178	1.7217	0.58190	1.7185	0.64239	1.7124
1	0.60860	1.5610	0.64328	1.5545	0.71336	1.5420
2	0.63541	1.4951	0.67474	1.4821	0.75555	1.4559
3	0.63989	1.4846	0.68286	1.4644	0.77242	1.4241
4	0.63917	1.4863	0.68549	1.4588	0.78368	1.4036
6	0.63395	1.4985	0.68673	1.4562	0.80244	1.3708
8	0.62783	1.5131	0.68689	1.4558	0.82119	1.3395
10	0.62176	1.5279	0.68691	1.4558	0.84103	1.3079
15	0.60737	1.5641	0.68692	1.4558	0.89803	1.2249
20	0.59428	1.5986	↓	↓	0.97125	1.1326
30	0.57211	1.6605			supercritical	
40	0.55512	1.7113			↓	
50	0.54252	1.7511				
60	0.53347	1.7808				
80	0.52264	1.8177				
100	0.51749	1.8358				
∞	0.51307	1.8516				

V. EXTRAPOLATION DISTANCE METHOD FOR A SLAB REACTOR

The slab reactor for the case of a thin core may also be treated by the extrapolation distance method in which the core is considered to be of zero thickness and the ratio of thermal flux to its derivative at the core-reflector interface is given by an extrapolation distance d. This method has been used by Ergen[8] for a spherical flux-trap reactor with slowing down by Fermi age theory and a thermally black core (d = 0). Here we correlate the extrapolation distance treatment for a slab core with the two-region treatment given in the previous section in order to find values for d and a constant denoted by p_{eff}, which will be defined below in connection with the criticality equation.

The diffusion equations in the reflector for the extrapolation distance treatment (E) are the same as for the method of Section IV in which the finite thickness of the core is treated explicitly (F). Thus the arbitrary constants in the solutions can be chosen so that the fluxes in the two methods are equal at the corresponding points in the reflector. This implies that the thermal extrapolation distance d for E must be the same as the ratio of thermal flux to its derivative at the core boundary for F. Therefore,

$$d = \frac{S_1 A \cosh \beta H + S_2 C \cosh mH}{S_1 A \beta \sinh \beta H + S_2 C\, m \sinh mH}$$

$$= \frac{1 - \dfrac{S_2}{S_1}\left(\dfrac{\beta \tanh \beta H + p_1}{m \tanh mH + p_1}\right)}{\beta \tanh \beta H - \dfrac{S_2}{S_1}\, m \tanh mH \left(\dfrac{\beta \tanh \beta H + p_1}{m \tanh mH + p_1}\right)} ,$$

where we have taken the case with $k_\infty < 1$ and written $|\ell| = \beta$. If the core has high thermal absorption, the value of d is given very roughly by

$$d \approx \frac{\coth mH}{m} .$$

In order to define p_{eff}, we integrate equations (1) to (4) over their regions of validity and write the criticality equation as given by (10) below. This gives

$$J_1 - \frac{D_1}{\tau}\left(1 + \tau B_\perp^2\right) I_{1c} + \frac{k_\infty}{p}\frac{D_2}{L_c^2} I_{2c} = 0 \qquad (6)$$

$$J_2 - \frac{D_2}{L_c^2}\left(1 + L_c^2 B_\perp^2\right) I_{2c} + p\frac{D_1}{\tau} I_{1c} = 0 \qquad (7)$$

$$-J_1 - \frac{D_1}{\tau}\left(1 + \tau B_\perp^2\right) I_{1r} = 0 \qquad (8)$$

$$-J_2 - \frac{D_2}{L_r^2}(1 + L_r^2 B_\perp^2)\, I_{2r} + \frac{D_1}{\tau} I_{1r} = 0 \qquad (9)$$

$$(\eta f p_{eff} - 1)\, J_2 - \frac{D_2}{L_r^2}(1 + L_r^2 B_\perp^2)\, I_{2r} - \frac{D_1}{\tau}\tau B_\perp^2 I_{1r} = 0 \qquad (10)$$

where

$$J_1 = D_1 \left.\frac{d\phi_{1r}^F}{dx}\right|_H = D_1 \left.\frac{d\phi_{1r}^E}{dx}\right|_0 ,$$

$$J_2 = D_2 \left.\frac{d\phi_{2r}^F}{dx}\right|_H = D_2 \left.\frac{d\phi_{2r}^E}{dx}\right|_0 ,$$

$$I_{1c} = \int_0^H \phi_{1c}^F\, dx ,$$

$$I_{2c} = \int_0^H \phi_{2c}^F\, dx ,$$

$$I_{1r} = \int_H^\infty \phi_{1r}^F\, dx = \int_0^\infty \phi_{1r}^E\, dx ,$$

$$I_{2r} = \int_H^\infty \phi_{2r}^F\, dx = \int_0^\infty \phi_{2r}^E\, dx .$$

The criticality equation (10) may be written more explicitly as

$$\frac{\eta f p_{eff}}{\tau p_1 (p_1 + p_2)(1 + d p_2)} = 1 . \qquad (11)$$

On combining equations (6), (7), (8), (9), and (10), we get

$$p_{eff} = \frac{1 - \frac{p}{k_\infty}\frac{D_1}{D_2}\frac{L_c^2}{\tau}(1 + \tau B_\perp^2)\frac{I_{1c}}{I_{2c}}}{1 + L_c^2 B_\perp^2 - p\,\frac{D_1}{D_2}\frac{L_c^2}{\tau}\frac{I_{1c}}{I_{2c}}} \qquad (12)$$

In equation (12), the terms involving $B_\perp^2$ allow for leakage from the outside of a core finite in the directions perpendicular to the x-axis. The other terms represent the fact that not all neutrons slow down in the

reflector and that there is a difference in the average number of neutrons thermalized per neutron slowing down in the core or in the reflector. For $B_I^2 = 0$ and H very small, the value of p_{eff} approaches one as expected.

VI. APPLICATION OF EXTRAPOLATION DISTANCE METHOD IN CYLINDRICAL GEOMETRY TO la_0 CORES

The theoretical treatment of the la_0-spaced lattices with B and W fuel is more difficult than that of the other lattices. Because of the close spacing of the fuel rods, it is difficult to calculate the core constants accurately. The epithermal absorption is so high that it may not even be reasonable to consider the low-energy flux as a Maxwellian plus a $1/E$ tail in determining cross sections. Also, because of the high resonance and epithermal absorption, the usual formulae for resonance or epithermal escape probabilities may be poor, as they are based on weak absorption. Because of these difficulties, complete calculations were not carried out for the la_0 lattices. However, the extrapolation distance model in cylindrical geometry was used to study important features of these lattices.

We consider a cylindrical reactor of finite height with a thin core at r = R and an infinite radial reflector. The radial diffusion equations in cylindrical coordinates are

$$D_1\left(\frac{d^2}{dr^2} + \frac{1}{r}\frac{d}{dr}\right)\phi_1 - \frac{D_1}{\tau}(1 + \tau B_z^2)\phi_1 + \frac{S}{2\pi R}\delta(r - R) = 0 \qquad (13)$$

$$D_2\left(\frac{d^2}{dr^2} + \frac{1}{r}\frac{d}{dr}\right)\phi_2 - \frac{D_2}{L_r^2}(1 + L_r^2 B_z^2)\phi_2 + \frac{D_1}{\tau}\phi_1 = 0 \quad . \qquad (14)$$

If we assume the extrapolation distance to have the same magnitude on both sides of the core, the solutions are

$$\phi_1(r) = \frac{S}{2\pi D_1} K_0(p_1 R) I_0(p_1 r) \quad , \quad r<R \quad ; \qquad (15)$$

$$\phi_1(r) = \frac{S}{2\pi D_1} I_0(p_1 R) K_0(p_1 r) \quad , \quad r>R \quad ; \qquad (16)$$

$$\phi_2(r) = \frac{S\,K_0(p_1 R)}{2\pi D_2 \tau (p_1^2 - p_2^2)}\left[\left(\frac{I_0(p_1 R) + dp_1 I_1(p_1 R)}{I_0(p_2 R) + dp_2 I_1(p_2 R)}\right) I_0(p_2 r) - I_0(p_1 r)\right] \quad , \quad r<R \quad ; \qquad (17)$$

$$\phi_2(r) = \frac{S\,I_0(p_1 R)}{2\pi D_2 \tau (p_1^2 - p_2^2)}\left[\left(\frac{K_0(p_1 R) + dp_1 K_1(p_1 R)}{K_0(p_2 R) + dp_2 K_1(p_2 R)}\right) K_0(p_2 r) - K_0(p_1 r)\right] \quad , \quad r>R \quad : \qquad (18)$$

The criticality equation is found from the relation

$$p_{eff}\eta f D_2 \left[\left.\frac{d\phi_2}{dr}\right|_{R_+} - \left.\frac{d\phi_2}{dr}\right|_{R_-} \right] + D_1 \left[\left.\frac{d\phi_1}{dr}\right|_{R_+} - \left.\frac{d\phi_1}{dr}\right|_{R_-} \right] = 0 \qquad (19)$$

to be

$$\frac{p_{eff}\eta f}{\left(1 - \frac{\tau}{L^2}\right)} \left[1 - p_2 R \left(K_0(p_1R) I_1(p_2R) \left(\frac{I_0(p_1R) + dp_1 I_1(p_1R)}{I_0(p_2R) + dp_2 I_1(p_2R)} \right) + I_0(p_1R) K_1(p_2R) \times \left(\frac{K_0(p_1R) + dp_1 K_1(p_1R)}{K_0(p_2R) + dp_2 K_1(p_2R)} \right) \right) \right] = 1 \quad . \qquad (20)$$

It may be seen on using the asymptotic forms of the Bessel functions[10] that, for very large R, the criticality equation is the same as for the slab reactor as it must be.

On the assumption that $p_{eff} \approx 1$, the total power is given by

$$\text{Power} = \frac{1}{3.2 \times 10^{16}} \frac{k_\infty}{\nu p} \quad \text{(Thermal Absorption in Core)}$$

$$= \frac{1}{3.2 \times 10^{16}} \frac{k_\infty}{\nu p} \frac{2S}{B_z(k_\infty/p)} = \frac{2S}{3.2 \times 10^{16} \nu B_z} \quad \text{Mw} \quad .$$

Thus the central flux for a total power of 100 Mw is

$$\phi_2(0) = \frac{B_z \nu (3.2 \times 10^{18})}{4\pi D_2 \left(1 - \frac{\tau}{L_r^2}\right)} K_0(p_1R) \left(\frac{I_0(p_1R) + dp_1 I_1(p_1R)}{I_0(p_2R) + dp_2 I_1(p_2R)} - 1 \right) n/(cm^2)(sec) \quad . \qquad (21)$$

We now use the above formulae to make some rough calculations for la_0 lattices with B and W fuel. Table XVI gives the results. The values of B_z^2 and R are experimental values[9] with R being the inner radius of cores which were less than 3 cm thick. In making the calculations, the numbers $\tau = 125$ cm^2, $L_r^2 = 1000$ cm^2, $D_2 = 0.75$ cm, and $\nu = 2.47$ were used.

Table XVI

CALCULATIONS FOR B AND W la_0 LATTICES

	R = 16.43 cm, B_z^2 = 0.00038 cm^{-2}			R = 26.22 cm, B_z^2 = 0.000535 cm^{-2}		
d (cm)	$p_{eff}\eta f$	$\frac{\phi_2(0)}{\phi_2(R_-)}$	$\phi_2(0)$* [n/(cm^2)(sec) x 10^{14}]	$p_{eff}\eta f$	$\frac{\phi_2(0)}{\phi_2(R_-)}$	$\phi_2(0)$* [n/(cm^2)(sec) x 10^{14}]
0	1.507	∞	20.1	1.479	∞	21.5
2	1.623	4.497	25.3	1.587	5.339	25.2
4	1.733	2.742	30.2	1.692	3.138	28.6
6	1.837	2.157	34.9	1.793	2.404	31.9

*Total power = 100 Mw

One would expect values of p_{eff} and d to be about the same for annular cores as for slab cores of the same thickness. This suggests that d should be about 4 cm for the cores of Table XVI, although this value is quite sensitive to L_c^2. As mentioned previously, it is difficult to calculate accurate constants for the la_0 core, so the value suggested for d may not be very good. The slab calculations indicate a value for p_{eff} of about 0.96 or 0.97. Combined with the values of $p_{eff}\eta f$ in Table XVI for d = 4, this gives values for ηf of the order of 1.75 or a little larger. The value of 1.75 is reasonable for thermal absorption alone, although epithermal absorption would tend to reduce it somewhat. However, a little smaller value of L_c^2, and consequently of d, would reduce the values of $p_{eff}\eta f$ in Table XVI. Also, the values of $p_{eff}\eta f$ are quite sensitive to τ and L_r^2, with an increase in τ or a decrease in L_r^2 increasing $p_{eff}\eta f$. In view of the sensitivity of equation (20) to the various constants involved and the uncertainty in these constants, about all that can be said is that the values of $p_{eff}\eta f$ in Table XVI are not inconsistent with experiment.

Table XVI shows that the flux peaking in the flux trap of la_0 lattices is very good, as would be expected because of the highly absorbing core. The central flux for a total power of 100 Mw is higher than that obtained with any of the $2a_0$ or $6a_0$ lattices.

APPENDIX

Equations Used in Fortran Program RE-240

The two-group radial diffusion equations in cylindrical coordinates are

$$D_{1c}\left(\frac{d^2}{dr^2}+\frac{1}{r}\frac{d}{dr}\right)\phi_{1c} - D_{1c}\left(\frac{1}{\tau}+B_z^2\right)\phi_{1c} + \frac{k_\infty}{p}\frac{D_{2c}}{L_c^2}\phi_{2c} = 0 \quad ,$$

$$D_{2c}\left(\frac{d^2}{dr^2}+\frac{1}{r}\frac{d}{dr}\right)\phi_{2c} - D_{2c}\left(\frac{1}{L_c^2}+B_z^2\right)\phi_{2c} + p\,\frac{D_{1c}}{\tau_c}\phi_{1c} = 0$$

in the core, and

$$D_{1r}\left(\frac{d^2}{dr^2}+\frac{1}{r}\frac{d}{dr}\right)\phi_{1r} - D_{1r}\left(\frac{1}{\tau_r}+B_z^2\right)\phi_{1r} = 0 \quad ,$$

$$D_{2r}\left(\frac{d^2}{dr^2}+\frac{1}{r}\frac{d}{dr}\right)\phi_{2r} - D_{2r}\left(\frac{1}{L_r^2}+B_z^2\right)\phi_{2r} + \frac{D_{1r}}{\tau_r}\phi_{1r} = 0$$

in the central reflector, with all notation used being standard.

For the flux-trap region, the solutions of the diffusion equations are

$$\phi_{1r} = AZ_1 \quad ,$$

$$\phi_{2r} = S_0 AZ_1 + BZ_2 \quad ,$$

where

$$Z_1 = I_0(p_{1r}r)$$

$$Z_2 = I_0(p_{2r}r)$$

$$p_{1r}^2 = \frac{1}{\tau_r} + B_z^2$$

$$p_{2r}^2 = \frac{1}{L_r^2} + B_z^2$$

$$S_0 = \frac{D_{1r}}{\tau_r D_{2r}\left(\frac{1}{L_r^2}-\frac{1}{\tau_r}\right)} \quad ,$$

and A and B are to be determined by boundary conditions.

The solutions of the diffusion equations in the core are

$$\phi_{1c} = CX + EY$$

$$\phi_{2c} = S_1 CX + S_2 EY \quad ,$$

where

$$X = J_0(\ell r) - \frac{J_0(\ell R_2)}{Y_0(\ell R_2)} Y_0(\ell r) \quad ,$$

$$Y = I_0(mr) - \frac{I_0(mR_2)}{K_0(mR_2)} K_0(mr) \quad ,$$

$$\ell^2 = \mu^2 - B_z^2 \quad ,$$

$$m^2 = \nu^2 + B_z^2 \quad ,$$

$$\mu^2 = 1/2 \left[- \left(\frac{1}{\tau_c} + \frac{1}{L_c^2} \right) + \sqrt{\left(\frac{1}{\tau_c} + \frac{1}{L_c^2} \right)^2 + \frac{4(k_\infty - 1)}{\tau_c L_c^2}} \right] \quad ,$$

$$\nu^2 = 1/2 \left[\left(\frac{1}{\tau_c} + \frac{1}{L_c^2} \right) + \sqrt{\left(\frac{1}{\tau_c} + \frac{1}{L_c^2} \right)^2 + \frac{4(k_\infty - 1)}{\tau_c L_c^2}} \right] \quad ,$$

$$S_1 = \frac{pD_{1c}}{\tau_c D_{2c} \left(\frac{1}{L_c^2} + \mu^2 \right)} \quad ,$$

$$S_2 = \frac{pD_{1c}}{\tau_c D_{2c} \left(\frac{1}{L_c^2} - \nu^2 \right)} \quad ,$$

R_2 is the outer radius of the core, and C and E are found from the boundary conditions.

At the core-reflector interface, the continuities of fast and thermal fluxes and of currents yield the critical determinant Δ and the constants A, B, C, and E. The critical determinant is given by

$$\Delta = S_2 \left(\frac{X'}{X} - \frac{D_{1r}}{D_{1c}} \frac{Z_1'}{Z_1} \right) \left(\frac{Y'}{Y} - \frac{D_{2r}}{D_{2c}} \frac{Z_2'}{Z_2} \right) - S_1 \left(\frac{X'}{X} - \frac{D_{2r}}{D_{2c}} \frac{Z_2'}{Z_2} \right) \left(\frac{Y'}{Y} - \frac{D_{1r}}{D_{1c}} \frac{Z_1'}{Z_1} \right) -$$

$$S_0 \frac{D_{2r}}{D_{2c}} \left(\frac{X'}{X} - \frac{Y'}{Y} \right) \left(\frac{Z_1'}{Z_1} - \frac{Z_2'}{Z_2} \right) = 0$$

where ' signifies d/dr and all functions are evaluated at the interface, r = R. Also,

$$\frac{B}{A} = \frac{\frac{Z_1}{Z_2}\left[S_2\left(\frac{X'}{X} - \frac{D_{1r}}{D_{1c}}\frac{Z_1'}{Z_1}\right) - S_1\left(\frac{Y'}{Y} - \frac{D_{1r}}{D_{1c}}\frac{Z_1'}{Z_1}\right) - S_0\left(\frac{X'}{X} - \frac{Y'}{Y}\right)\right]}{\left(\frac{X'}{X} - \frac{Y'}{Y}\right)} ,$$

$$\frac{C}{A} = \frac{Z_1}{X}\left(\frac{D_{1r}}{D_{1c}}\frac{Z_1'}{Z_1} - \frac{Y'}{Y}\right)\Bigg/\left(\frac{X'}{X} - \frac{Y'}{Y}\right)$$

$$\frac{E}{A} = \frac{Z_1}{Y}\left(\frac{X'}{X} - \frac{D_{1r}}{D_{1c}}\frac{Z_1'}{Z_1}\right)\Bigg/\left(\frac{X'}{X} - \frac{Y'}{Y}\right) .$$

The average fluxes are

$$\bar{\phi}_{1r} = \frac{4A}{\pi}\frac{I_1(p_{1r}R)}{p_{1r}R} ,$$

$$\bar{\phi}_{2r} = \frac{4A}{\pi}\left[\frac{S_0 I_1(p_{1r}R)}{p_{1r}R} + \frac{B}{A}\frac{I_1(p_{2r}R)}{p_{2r}R}\right] ,$$

$$\bar{\phi}_{1c} = \frac{4A}{\pi(R_2^2 - R^2)}\left[\frac{C}{A}\cdot\frac{1}{\ell^2}\left(RX' + \frac{2}{\pi Y_0(\ell R_2)}\right) + \frac{E}{A}\cdot\frac{1}{m^2}\left(-RY' + \frac{1}{K_0(mR_2)}\right)\right] ,$$

$$\bar{\phi}_{2c} = \frac{4A}{\pi(R_2^2 - R^2)}\left[\frac{S_1 C}{A}\cdot\frac{1}{\ell^2}\left(RX' + \frac{2}{\pi Y_0(\ell R_2)}\right) + \frac{S_2 E}{A}\cdot\frac{1}{m^2}\left(-RY' + \frac{1}{K_0(mR_2)}\right)\right] ,$$

where X' and Y' are evaluated at r = R. In order to assign a value to the constant A, the normalization condition

$$\frac{k_\infty}{p}\frac{D_{2c}}{L_c^2}\bar{\phi}_{2c} = 1$$

was used.

Input for the RE-240 program consists of the core and reflector material constants, axial buckling, core outer radius, and two guesses for the inner radius R of the core. The critical determinant is evaluated for these two values of R and (N - 2) other values found by interpolation where $2 \le N \le 9$ and N is an input number. The output consists of the N values of R and Δ, the average fast and thermal fluxes in core and reflector, the values of the fluxes on the reactor axis and at the core-reflector interface, and miscellaneous other data concerning the fluxes.

ACKNOWLEDGMENTS

The author would like to thank Jerry Rathbun for writing the Fortran program RE-240 used in the $6a_0$ calculations, and Larry Noble for carrying out some of the desk computer calculations.

REFERENCES

1. W. C. Redman, J. A. Thie, and L. R. Dates, Hazards Summary Report on the Oxide Critical Experiments, ANL-5715 (April 1957).

2. W. C. Redman et al., Critical Experiments with Thoria-Urania Fuel in Heavy Water, ANL-6378 (to be published).

3. K. E. Plumlee and S. G. Kaufmann, Flux to Fission Ratios in Annular Cores, Transactions of the American Nuclear Society, 2 (1), 166 (June 1959).

4. K E. Plumlee, ANL report on flux-trap experiments in ZPR-VII, to be published.

5. M. K. Butler and J. M. Cook, Univac Programs for the Solution of One Dimensional Multigroup Reactor Equations, ANL-5437.

6. Reactor Physics Constants, ANL-5800, p. 161.

7. C. N. Kelber and P. Kier, Few Group Analysis of D_2O-U^{235} Assemblies, Nuclear Science and Engineering 8 (1) 1 (July 1960).

8. W. K. Ergen, The Highest Thermal Neutron Fluxes Obtainable from Fission Reactors, Proceedings of the United Nations International Conference on the Peaceful Uses of Atomic Energy, Geneva, Switzerland, 10, 181 (1955).

9. K. E. Plumlee, private communication.

10. British Association for the Advancement of Science Mathematical Tables, Volume VI Bessel Functions, Part I, Cambridge (1950).